

Efficient Compilation for Shuttling Trapped-Ion Machines via the Position Graph Architectural Abstraction

Bao Bach

Computer and Information Sciences
Quantum Science and Engineering
University of Delaware
US
baobach@udel.edu

Ilya Saфро

Computer and Information Sciences
Physics and Astronomy
University of Delaware, US
isafro@udel.edu

Ed Younis

Computational Research Division
Lawrence Berkeley National
Laboratory, US
edyounis@lbl.gov

ABSTRACT

With the growth of quantum platforms for gate-based quantum computation, compilation holds a crucial factor in deciding the success of the implementation. There has been rich research and development in compilation techniques for the superconducting-qubit regime. In contrast, the trapped-ion architectures, currently leading in robust quantum computations due to their reliable operations, do not have many competitive compilation strategies. This work presents a novel unifying abstraction, called the position graph, for different types of hardware architectures. Using this abstraction, we model trapped-ion Quantum Charge-Coupled Device (QCCD) architectures and enable high-quality, scalable superconducting compilation methods. In particular, we devise a scheduling algorithm called SHuttling-Aware PERmutative heuristic search algorithm (SHAPER) to tackle the complex constraints and dynamics of trapped-ion QCCD with the cooperation of state-of-the-art permutation-aware mapping. This approach generates native, executable circuits and ion instructions on the hardware that adheres to the physical constraints of shuttling-based quantum computers. Using the position graph abstraction, we evaluate our algorithm on theorized and actual architectures. Our algorithm can successfully compile programs for these architectures where other state-of-the-art algorithms fail. In the cases when other algorithms complete, our algorithm produces a schedule that is 14% faster on average, up to 69% in the best case.

Reproducibility: source code and computational results are available at [will be added upon acceptance].

CCS CONCEPTS

• **Computer systems organization** → **Quantum computing**; • **Software and its engineering** → **Abstraction, modeling and modularity**; **Compilers**.

KEYWORDS

Quantum compilation, Trapped-ion architecture, Quantum charge-coupled devices, Quantum circuit mapping

1 INTRODUCTION

Quantum computing is rapidly evolving into a transformative technology with significant potential in areas such as finance [26], simulations in chemistry [9], combinatorial optimization [60], and machine learning [4] to mention just a few. We are currently in the *noisy intermediate-scale quantum* (NISQ) computing era, characterized by quantum devices with tens to thousands of noisy qubits,

short coherence times, and limited connectivity. One of the key challenges in this era is the efficient compilation of quantum circuits to address the specific limitations and architectural constraints of various quantum hardware platforms.

Among the various quantum computing architectures, *trapped-ion* (TI) devices stand out as one of the most promising options, arguably offering the most robust computation. These devices confine atomic ions within traps and utilize two of the atomic states to represent quantum information. Operations are executed using precisely calibrated lasers that are directed at the trap. The unique physics of trapped-ion architectures allows for high-fidelity operations and long coherence times at the cost of long execution times. For example, trapped-ion operations are measured in microseconds, whereas superconducting machine instructions are measured in nanoseconds [36]. To make this matter worse, in the current state-of-the-art architecture scheme called *quantum charge-coupled device* (QCCD), the trapped ions must be physically shuttled around the chip during program execution to create connections. Figure 1 demonstrates an example of QCCD architecture and the use of shuttling operations to move ions around. These slow shuttling operations comprise most of the final program’s runtime. As a result, establishing high-quality compilation practices for TI devices is absolutely crucial.

The current compilation paradigm employed for TI systems usually involves a two-layer approach [33, 57]. First, the logical layer abstracts away the device’s unique physical constraints by assuming all qubits are connected in a simple all-to-all model. Here, compilers focus on optimizing a program in a machine-agnostic way. The second compilation step is then to resolve the physical constraints given the logical program. This involves breaking the logical operations up with shuttling instructions to create a schedule of shuttling instructions. While this all-to-all assumption simplifies some aspects of the compilation process, it paradoxically complicates the ability to accurately and effectively account for the underlying hardware’s unique constraints. We argue that this two-layer approach is not well-suited for producing efficient shuttling schedules that minimize execution time and, as a result, maximize reliability. This is because the hardware-agnostic stage does not consider shuttling and may introduce a seemingly great optimization only to make it worse during shuttling. For example, during the circuit optimization step, gates that act on the far-distance and nearby ions will be indistinguishable. This can lead to accumulated far-distance ion coupling, which introduces underlying overhead in the shuttling stage. Consequently, there is a pressing need to break away from the limitations imposed by the two-layer approach and formulate a

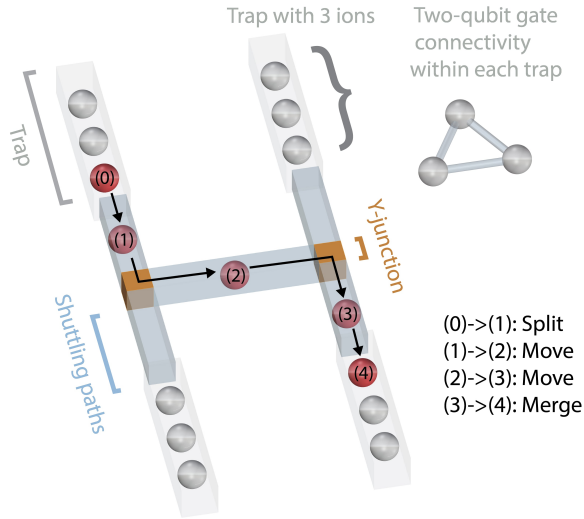


Figure 1: The H-type [29, 45] QCCD-based trapped-ion architecture. Here the ion is moved from one trap to another trap using 3 shuttling operations. Move (0 → 1) denotes a split operation to split the ion from the trap. Move (1 → 2) and (2 → 3) denotes move through Y-junction (T-junction) into segment space. Finally, move (3 → 4) shows the merge operation of the ion into the new trap.

more meaningful abstraction of the constraints and shuttling operations inherent to QCCD architectures. However, this presents several challenges as the complex constraints yielded by the physical architectures cannot be captured on the well-known coupling graph abstraction [62], and there is a lack of physical abstraction for the shuttling-based compilation schedule. Introducing an effective abstraction that can lead to more efficient compilation schemes for QCCD-based shuttling architecture is extremely important. This work attempts to address the following fundamental question: *How do we break the assumption of all-to-all qubit connectivity and its resulting two-stage approach to TI compilation, and instead derive a meaningful abstraction for the constraints and shuttling operations of QCCD architectures for the compilation process?*

Compilers for superconducting devices abstract the entire architecture to a coupling graph, which reflects the physical connectivity of the qubits [62]. That is, multi-qubit gates can only be applied to qubits connected in the graph. All other machine-level details are abstracted away, and as a result, there have been numerous algorithms developed for compiling these graphs. In this paper, we introduce the *position graph*, an extension to the coupling graph abstraction, as the answer to the posed question and a unifying abstraction between different architecture types. This abstraction provides a framework for encoding hardware constraints while enabling the same superconducting algorithms to be trivially adapted for the QCCD case. The position graph is a thin middle-layer abstraction in the quantum compilation stack, allowing for broader applicability of compilers. We argue that this abstraction naturally implies physical restrictions of the shuttling operations and QCCD

system, as will be discussed in Section 3. Moreover, the initial mapping of logical qubits to physical ions and the transitions of physical ions between traps using shuttling operations can be generalized through this abstraction.

To demonstrate the efficacy of our proposed abstraction, we successfully port a state-of-the-art mapping algorithm for superconducting qubits to our position graph representation. Our findings indicate that this adaptation competes effectively with existing shuttling algorithms and enhances them by handling a wider range of cases. In particular, our approach is compatible with any gate set and offers solutions for congestion issues without oversimplifying the hardware constraints. While other approaches either fail to resolve the deadlocks created by shuttling operations or try to simplify the constraints making them unusable in practice, our proposed *SHuttling-Aware PERmutative search algorithm* (SHAPER) resolves scenarios where the state-of-the-art fails. In more detail, given a QCCD-based TI system with m traps with each having a maximum ion capacity of n , our *position graph*-based method manages to compile any quantum circuit with mn qubits. In contrast, state-of-the-art tools can only compile circuits with $(m - 1)n$ qubits.

In summary, our contributions are:

- (1) We introduce the *position graph* abstraction to bridge the gap between the rich literature in circuit mapping problems and the shuttling problem in TI systems. To the best of our knowledge, this is the first attempt to narrow the difference between different quantum architecture abstractions which has the potential to unify compilation processes for various architectures.
- (2) We propose SHuttling-Aware PERmutative search algorithm (SHAPER) to prove the usefulness of the *position graph* by porting a state-of-the-art mapping algorithm from superconducting systems. The algorithms are benchmarked across various quantum circuits and architectures, demonstrating successful results across all configurations where the state-of-the-art methods fail. For executable configurations, our approach consistently delivers superior performance in most cases.
- (3) We demonstrate the first shuttling-based algorithm that can resolve congestion and deadlocks as well as fully utilize two-dimensional QCCD-based architectures.

The rest of the paper is organized as follows. Section 2 gives a brief introduction to quantum information, quantum compilation, and permutation-aware mapping strategy. Section 3 introduces the Quantum Charge-coupled device (QCCD) system, the shuttling operations, and their constraints. Sections 4 and 5 introduce the *position graph* abstraction and mapping algorithm that is based on it, which are the main novel points of the paper. We present the evaluation of the proposed algorithm in section 6. Related work is presented in Section 7. We conclude our paper with a discussion in Section 8.

2 QUANTUM INFORMATION AND COMPILATION

2.1 Quantum Information

The fundamental information unit of quantum information is a quantum bit or *qubit* for short, which represents a quantum state that belongs to the Hilbert space spanned by two basis states. For computation, these basis quantum states are $|0\rangle$ and $|1\rangle$, represented by the vectors $\begin{bmatrix} 1 \\ 0 \end{bmatrix}$ and $\begin{bmatrix} 0 \\ 1 \end{bmatrix}$, respectively. A qubit, $|\psi\rangle$ is then represented as a superposition of these: $|\psi\rangle = \alpha|0\rangle + \beta|1\rangle = \begin{bmatrix} \alpha \\ \beta \end{bmatrix}$, where the amplitudes $\alpha, \beta \in \mathbb{C}$ and $|\alpha|^2 + |\beta|^2 = 1$. When measuring the quantum state, the probability of receiving state $|0\rangle$ is $|\alpha|^2$, and state $|1\rangle$ is $|\beta|^2$, respectively. Composing multiple qubits together in an n -qubit system creates a superposition state over all n -bit strings, formally defined as $|\Psi\rangle = \sum_{i=0}^{2^n-1} \alpha_i |i\rangle$ where $\alpha \in \mathbb{C}^{2^n}$ and $\sum_{i=0}^{2^n-1} |\alpha_i|^2 = 1$. After measurement, state $|i\rangle$ is received with probability $|\alpha_i|^2$.

A quantum state is transformed by matrix operators that maintain the previously mentioned constraints. By definition, these linear transformations belong to the unitary group $U(2^n)$, where n is the number of qubits transformed. While any *unitary* is a valid state transformation, each quantum hardware architecture provides a small, fixed set of natively executable operations due to engineering and physical constraints. Quantum computers that are *universal* can implement any operation with a sequence of their native instructions. These native instructions are typically referred to as *gates* and described compactly by small unitary operators. In the context of the trapped-ion system, the native set varies slightly by vendor. In the case of Quantinuum [20], the native gates are:

$$RZ(\theta) = \begin{bmatrix} e^{-i\frac{\theta}{2}} & 0 \\ 0 & e^{i\frac{\theta}{2}} \end{bmatrix}, \quad (1)$$

$$U1q(\theta, \phi) = \begin{bmatrix} \cos(\frac{\theta}{2}) & -ie^{-i\phi} \sin(\frac{\theta}{2}) \\ -ie^{i\phi} \sin(\frac{\theta}{2}) & \cos(\frac{\theta}{2}) \end{bmatrix} \text{ and} \quad (2)$$

$$Rzz(\theta) = \begin{bmatrix} e^{-i\frac{\theta}{2}} & 0 & 0 & 0 \\ 0 & e^{i\frac{\theta}{2}} & 0 & 0 \\ 0 & 0 & e^{i\frac{\theta}{2}} & 0 \\ 0 & 0 & 0 & e^{-i\frac{\theta}{2}} \end{bmatrix}. \quad (3)$$

Finally, quantum programs are expressed in the *circuit model* consisting of (1) initialization of qubits depicted as wires going left to right through time, (2) quantum gates evolving the state of the qubits they touch, and (3) measurements resulting in the final readout. Without considering the measurement and initialization, the complete function a quantum circuit implements can be represented by the unitary matrix U resulting from properly multiplying all gate operations [47]. We say that two quantum circuits are equivalent if they implement the same unitary matrix U up to a *global phase* – a complex factor with magnitude one.

2.2 Quantum Compilation

In the context of quantum computing, the term “compilation” often refers to the process of transforming a given “logical” quantum

circuit (i.e., the quantum algorithm) into an equivalent, natively-executable circuit given a specific quantum processing unit (QPU). Compilers must overcome challenges such as limited qubit connectivity, gate fidelity, and other hardware-specific constraints in this essential task. Additionally, effective compilation enhances the performance of quantum algorithms and reduces errors by minimizing resource utilization. The Noisy Intermediate-Scale Quantum (NISQ) era requires these steps, as high gate error rates and limited coherence times currently characterize devices. Therefore, compilation’s primary goal is to reduce instruction counts and execution time. The two main processes in quantum compilation are transpilation and circuit mapping.

Transpilation. The goal of transpilation is to retarget the original circuit into one that only uses gates from the native gates set given a target QPU. In quantum computing, each platform has its own set of universal gates. For instance, superconducting platform [31] has the universal gate set of SX , RZ , and $CNOT$, while trapped-ion platform [29] has the universal gate set of RZ , $U1q$, and RZZ . State-of-the-art methods for transpilation involve re-synthesizing partitioned subcircuits from a larger circuit [68]. Here, large circuits are first partitioned into blocks of fixed sizes by grouping adjacent gates. Then, the unitaries for each block are calculated and re-synthesized in the new gate set using one of many different algorithms.

Circuit Mapping. Circuit mapping, also known as routing and layout, is responsible for overcoming the connectivity constraints of a quantum architecture. This compilation step is usually mentioned in the context of superconducting architectures, where physical qubit connections are defined by a coupling graph, and multi-qubit gates can only be physically operated between connected qubits. Therefore, routing operations, such as a SWAP gate, must be chained to map a physically distant logical operation to a sequence of physical gates. Although necessary, this compilation procedure can greatly increase the execution time and gate count of a program and, therefore, is the most important to optimize. To minimize the overhead, circuit mapping algorithms such as [3, 34, 41] are used to (1) derive the best initial mapping from logical qubits (from the original circuit) to the physical qubits (from the hardware architecture) and (2) perform intermediate mapping transition to remap the far-distance qubits to physically-coupled qubits. In the QCCD-based TI platform, the shuttling process is similar to this mapping process. The difference is that shuttling utilizes a variety of ion shuttling operations, which physically move the ion, rather than logical SWAP gates, which mathematically move a qubit’s state.

2.3 Permutation-Aware Mapping

The *permutation-aware mapping* (PAM) is a state-of-the-art technique for mapping quantum circuits to superconducting devices [38]. It is based on the topology- and permutation-aware synthesis principles, as well as the mapping heuristic, such as SABRE [34]. We expand on these principles in this work and, therefore, introduce them here.

Topology-aware synthesis. Quantum circuit synthesis finds a quantum circuit that implements a given target unitary matrix. This process is made topology-aware when the resulting circuit is already mapped to a target QPU’s topology or coupling map.

The topology-aware quantum circuit synthesis algorithms in recent years have the following intuition: by ‘enumerating’ the space of possible solutions, in our case, the space of possible circuits, the desired solution can be found by searching the space. Specifically, Qsearch [13] performs the space enumeration through tree construction. Each branch constitutes a possible gate operation on specific qubits with the root node as the initial layer. Branches not directly mappable to hardware are pruned, providing the topology-awareness. After the construction, a search algorithm is deployed to find the desired node in the tree that satisfies optimality criteria. As Qsearch steps over a candidate solution, it employs a numerical optimizer to find the best parameters for that structure.

Permutation-aware synthesis. Following this line of research, [38] introduces permutation-aware synthesis (PAS). PAS makes two observations toward better synthesis. First, classically permuting qubit indices during initialization and readout is a trivial process. Second, given a unitary matrix U , one of its classically-resolvable permutations, P_oUP_i for some permutations P_o, P_i , may be easier to synthesize and require fewer quantum resources. To this effect, when synthesizing a unitary matrix U , it will enumerate all possible permutations and introduce them in the circuit. The permutations are introduced as an identity since $PP^T = I$ for all permutations P . This results in $P_o^T P_o U P_i P_i^T = U$. The outer permutations are factored out to the qubit initialization and readout stages, and $P_o U P_i$ is left to synthesize. This process produces very resource-efficient circuits and, in some cases, leads to circuits using fewer resources than provable-optimal circuits since it breaks the assumptions of the proof.

Heuristic mapping. Heuristic mapping algorithms walk the circuit gate-by-gate and insert swaps determined by a heuristic to make the next gate or set of gates executable. The canonical algorithm is SABRE [34], which divides the circuit into the front and extended layers. The *front layer* consists of the minimal nodes in a topological ordering, and the *extended layer*, representing a lookahead window, consists of some configurable number of gates after the front layer. Its heuristic determines which swap to insert next by balancing the routing cost for the gates in the front layer with gates in the extended layer. To perform layout, this routing procedure is repeated in reverse, often multiple times, with the final ordering providing a good starting layout.

Permutation-aware mapping. Permutation-aware mapping (PAM) [38] combines the concepts of heuristic mappers with permutation-aware synthesis. To introduce PAS into the mapping process, a large circuit is first partitioned into small synthesizable blocks. These blocks are then synthesized for every permutation and stored. The SABRE mapping algorithm then proceeds with a generalized heuristic for blocks rather than gates. When a block in the front layer is made executable and moved off the front layer, another heuristic is performed that selects the best permutation of the block. PAM resolves the introduced outer permutations by merging them with the current state of the qubit mapping. As a result, PAM’s heuristic balances the number of gates in the synthesized permutation with the effect the permutation will have on the rest of the mapping process.

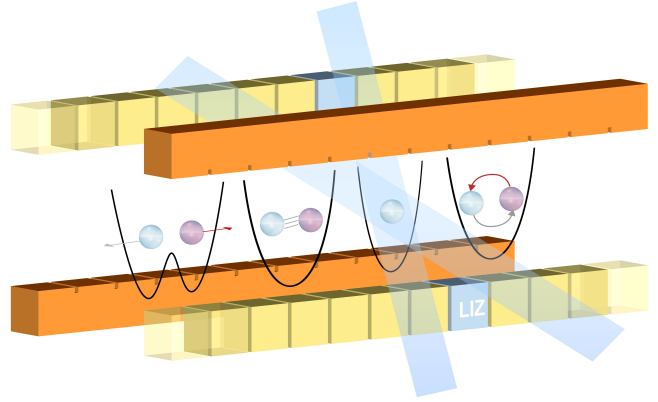


Figure 2: Linear QCCD trapped ion architecture with shuttling operations where the atomic ions are stored in different segments. The figure illustrates common reconfiguration operations of the ion positions: (1) split group of ions, (2) merge ions into a group, (4) physically swap ions. Furthermore, the blue zone at (3) indicates that operations performed on this ion in this specific trap are executable.

3 QUANTUM CHARGE-COUPLED DEVICE

Trapped-ion (TI) platforms for quantum computation have drawn significant attention due to their robustness and seemingly all-to-all connectivity, leading to their widespread use in the NISQ era. Compared with its competitors, such as superconducting-qubit systems, the TI system is known to not suffer from the connectivity challenge, which is a massive hindrance in superconducting systems [30]. However, trapped-ion architectures face a scaling issue. As a single trap’s ion count increases, so does its heating, presenting difficulties in ion control and gate implementation for long ion chains. This heating is directly related to a system’s fidelity [67].

To tackle this problem, the Quantum Charge Coupled Device (QCCD) model was proposed [29] as a modular and scalable trapped-ion architecture, where small traps are connected through ion shuttling paths. In more detail, the QCCD-based TI system consists of multiple small capacity traps, as well as, segments and junctions providing pathways for the ions to move from trap to trap. Figure 2 illustrates an example of a QCCD architecture. By restricting the trap size capacity, QCCD design achieves fast, high-fidelity two-qubit operations within each trap. Figure 1 illustrates the shuttling process as an ion physically moves from one trap to another. Currently, many state-of-the-art TI systems [14, 42, 44, 52, 64] and the future development roadmap of TI vendors [53] are built based on the concept of QCCD.

Effectively, the QCCD design trades the scaling issue for a connectivity challenge, as the all-to-all model is only available for ions within the same trap. This trade-off is desirable as the scaling issue prevents long-term adoption, whereas resolving shuttling schedules becomes a compiler stage. However, hardware vendors have continued to uphold an illusion of all-to-all connectivity between any qubit [54]. This creates an inefficient compiler stack as, first, a program is optimized without concern for the QCCD architecture. Only after this stage, is a shuttling sequence resolved. This can lead

to inefficient circuits since the first step may perform a seemingly great optimization, which will lead to more shuttling operations in the second compilation stage. Since shuttling operations account for a majority of the compute time, they must be minimized with the highest priority. For example, a movement operation between junctions may require around 100 to 120 microseconds [24] whereas a gate operation only requires 30 to 100 microseconds [2, 22].

Moreover, QCCD architecture also introduces specific constraints related to gate execution. As depicted in Figure 2, ions must be moved to an executable zone for gate operations. To represent this constraint, we assume two trap types exist: executable and storage traps. Therefore, the following constraints are established (1) single-qubit gates can be employed on ions in executable traps, and (2) multi-qubit gates can only be applied to ions existing in the same executable trap. Besides these constraints, moving physical ions between traps using shuttling operations also imply restrictions [39, 45, 57] that we specify as follows

- (1) Only one ion can exist on a segment simultaneously.
- (2) At a given time, only one ion can pass through a junction.
- (3) Traps cannot contain more ions than their maximum capacity.
- (4) The *split* operation removes the outermost ion from a trap into a connected segment.
- (5) The *merge* operation adds an ion from a junction to the outermost position in a trap.
- (6) The *move* operation moves an ion from one segment to another, passing through a junction.
- (7) The *shuttling* operations can be executed in parallel as long as there is no collision.
- (8) Gate operations on different traps can be executed in parallel.

The above restrictions are usually not considered during the circuit optimization stages due to their complexity in resolving congestion. Figure 3 depicts an example of congestion when trying to move q_2 to the same trap as q_3 . In this case, we unintentionally create congestion as we q_2 cannot be merged into the trap, and free space cannot be made trivially.

4 POSITION GRAPH ABSTRACTION

We introduce a novel abstraction called the *position graph*, which abstracts a QCCD-based TI system’s physical architecture using the graph language [55]. The position graph breaks the all-to-all connectivity assumption, offering a more expressive representation of the shuttling constraints in a structural and meaningful way. Figure 4 provides an example of a position graph. The position graph is a generalization of the coupling graph for superconducting compilation and provides a unifying abstraction over different hardware architectures. The numerous algorithms for mapping programs to superconducting devices can be trivially ported to this abstraction, enabling them to reason about the complex constraints of the QCCD model easily.

First, we give the formal definition of position graph as presented in Definition 1. Given the hardware architecture, the sets of junctions \mathbf{J} and segments \mathbf{S} , the position graph $G_P(\mathbf{V}, \mathbf{E}, \psi)$ is an abstraction that can (1) fully express the architecture of the physical structure, (2) naturally enforce the constraints of QCCD-based

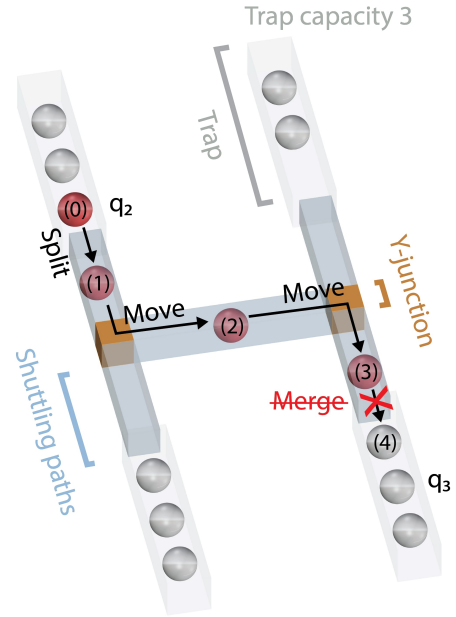


Figure 3: An example of congestion created when trying to move q_2 to the same trap with q_3 . Here, after moving q_2 next to the trap containing q_3 , the merge operation fails due to not enough free space in the trap. The congestion is created as q_3 can not be merged into the trap and there is no one-step shuttling operation to free space on the q_3 trap.

TI system and (3) indicate the current state of the system when combining with ion assignment Φ .

DEFINITION 1 (POSITION GRAPH). Given the hardware architecture with (1) the set of ion traps \mathbf{T} , $|\mathbf{T}| = \mathbf{m}$, where each trap $t \in \mathbf{T}$ has a capacity of \mathbf{n}_t ions, (2) the set of junctions \mathbf{J} , and (3) the set of segments \mathbf{S} . We define the Position Graph $G_P(\mathbf{V}, \mathbf{E}, \psi)$ where \mathbf{V} is the set of vertices, \mathbf{E} is the set of edges, and $\psi : \mathbf{E} \rightarrow \mathbf{L}_E$ is the labeling function that assigns labels to edges from the set \mathbf{L}_E . A node $i \in \mathbf{V}$ corresponds to a possible position of an ion in the device at some time. (For example, in the QCCD devices, the ions could be either within the traps or the shuttling paths as depicted in Figure 4). An edge $ij \in \mathbf{E}$ corresponds to a possible transition of an ion from position $i \in \mathbf{V}$ to $j \in \mathbf{V}$. (For example, in the QCCD devices, the transition corresponds to the shuttling operation.) Therefore,

$$|\mathbf{V}| = \sum_{t \in \mathbf{T}} \mathbf{n}_t + |\mathbf{S}| \quad (4)$$

$$|\mathbf{E}| = \sum_{t \in \mathbf{T}} (\mathbf{n}_t - 1) + \sum_{j \in \mathbf{J}} \frac{d(j)(d(j) - 1)}{2} + |\mathbf{JT}| - |\mathbf{JJ}| \quad (5)$$

where j denotes a junction, \mathbf{JT} denotes the set of segments connecting junctions and traps, \mathbf{JJ} denotes the set of segments connecting pairs of junctions, and $d(j)$ denotes the degree of junction j (see examples in Figures 4 and 5). The set of edge labels is defined as dedicated to the QCCD architecture

$$\mathbf{L}_E = \{\text{swap, merge/split, move}\} \quad (6)$$

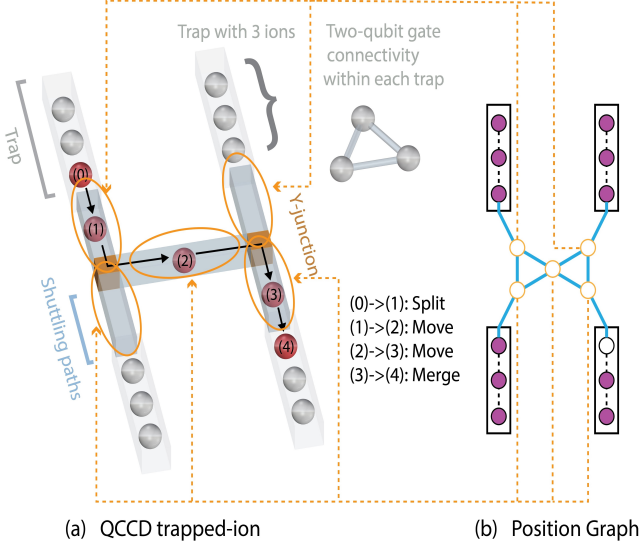


Figure 4: Example of mapping a QCCD-based TI architecture to its corresponding position graph. Here, each *position* in the shuttling paths is mapped to an orange node of the graph, while each available space in a trap, according to the trap’s capacity, is also mapped to a node in the position graph. The edges of the position graph are labeled with a shuttling operation such as split, merge, move, and inner swap between ions inside the same trap. When a node is filled (colored purple), it indicates the existence of an ion in that specific space.

includes the types of ion transitions within and outside of the trap. The **swap** label corresponds to the transition between available space inside the trap zone. The **merge/split** label corresponds to the transition between available spaces inside and outside the trap zone, and the **move** label corresponds to movement between available spaces outside the trap zone.

As depicted in Figure 4, the physical QCCD-based TI architecture is represented by a position graph which is similar to the connectivity graph but has many foundational differences. Here, QCCD architecture contains 4 traps each of a maximum capacity of 3 ions, the set of junctions J contains 2 junctions, and the set of segments S contains 5 shuttling paths. Thus, in this case, the hardware architecture can be abstracted to G_p with 17 nodes and 18 edges.

Note that in Definition 1, each node of the position graph is not described as an ion or qubit like the physical connectivity graph, but it describes a possible space that ions can be moved into. Similarly, for the shuttling path, we describe a shuttling path as a node in a position graph that characterizes the constraint that only one ion can appear in the shuttling path at a given time. With this definition, the edge of the position graph naturally stands for a move between available spaces (which is a shuttling operation that moves the ions between two spaces in the physical system). According to Definition 1: (1) the edges between spaces within the trap labeled as **swap** correspond to the inner swaps between pairs

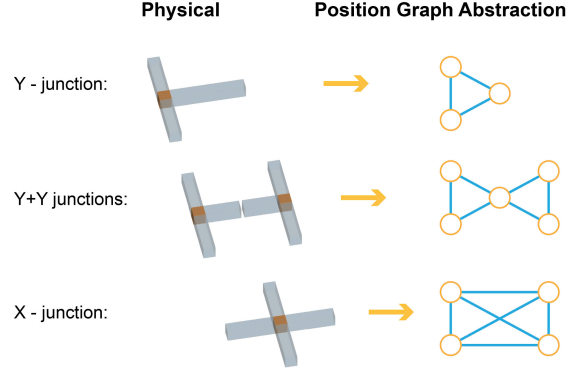


Figure 5: Mapping physical junction to its position graph abstraction. The figure shows how the Y-junction (T-junction), X-junction, and combination of Y-junction (T-junction) are transformed into abstraction.

of ions (also called chain reordering in [45]); (2) the edges between spaces inside the trap zone and outside the trap zone, labeled as **merge/split**, indicate either merge or split operation; and (3) edges between spaces outside trap zone, labeled as **move**, reflect the move operation between junctions.

4.1 Encoding QCCD into Position Graph

From a physical QCCD architecture, the position graph can be easily constructed by consecutively going through all the traps, junctions, and shuttling paths. First, traps with capacity n imply that there are n available spaces within that trap to store up to n ions. As shown in 4, to represent this in the position graph, we use the n -linear space where the edges connecting these nodes are labeled as **swap**. Next, we consider each junction and create its representation in the position graph according to the junction’s degree. A d -degree junction creates a complete subgraph with d nodes for the position graph. The motivation behind this is due to the characteristic of d -degree junction that creates all-to-all connections between d spaces (i.e., it allows pairwise connectivity between all the spaces). The nodes created by junctions are connected with the edges that are labeled as **move**. If two junctions are connected through a shuttling path, we can merge them through a node without destroying the meaning as shown in Figure 5. After this, we need to create edges that connect the disconnected components (traps and junctions) with respect to their connections in the physical architecture (the segments), labeled as **merge/split**. The edges that connect the components are assured to reflect the shuttling operations.

4.2 States of Position Graph

Given G_p , a feasible assignment of ions Φ constitutes the state of the position graph. The ion assignment $\Phi : Q \rightarrow V$, where Q is the set of logical qubits, maps the logical qubits from the original quantum circuit to the position (node) in the position graph. Legal shuttling

operations change the states. For example, Figure 6 displays the change of state in the position graph caused by the change in ion assignment Φ after each shuttling operation when moving q_2 to the trap containing q_3 . Enforcing that no ion swap can happen outside of the trap zone naturally forms the constraint of junctions and shuttling paths and reflects congestion. An example of how the position graph exhibits congestion and imposed constraints is shown in Figure 7. Here we want to move q_2 to the trap that contains q_3 , for gate execution at (q_2, q_3) . However, a blockage with q_5 will surely create congestion if not moved, as demonstrated in Figure 3. This is clearly exhibited by the architectural abstraction from the position graph where there is no valid move to trap containing q_3 .

5 POSITION GRAPH COMPILATION

Given the encoding of QCCD-based TI architecture into the position graph, the similarity between solving the circuit mapping problem (i.e., from the connectivity graph of the superconducting qubit system) and solving the shuttling schedule (i.e., from the position graph of the QCCD-based TI) becomes more evident. In the superconducting qubit case, given the entanglement graph from the quantum circuit, we apply the SWAP operation to minimize the distance between qubits that are far from each other in the connectivity graph but near each other in the entanglement graph (having many two-qubit gates applying on those qubit pairs). Similarly, in the TI QCCD case, we try to perform the transition of ions through shuttling operations to close the distance between ions that are far in the position graph but need to be in the same trap for execution.

From this alignment, it is tempting to treat the position graph of the trapped-ion system analogously to the connectivity graph of a superconducting system, thereby leveraging the established circuit mapping algorithms. However, this is not straightforward due to the fundamental differences in the constraints of superconducting and TI technologies. While superconducting mapping allows moving qubits next to each other for coupling through SWAP, trapped ions mapping does not allow direct swap between two ions outside of the trap zone and there exists deadlock situations where the wanted movement is prohibited.

5.1 Shuttling-Aware Heuristic Search

To tackle the shuttling and mapping problem on the QCCD-based TI system, we devise a novel mapping algorithm that is inspired by the well-known SWAP-based Bidirectional heuristic search algorithm (SABRE) [34] and permutation-aware mapping (PAM) [38]. Adapting these ideas to shuttling-based devices and position graph architectural abstraction, we introduce the SHuttling-Aware PERmutative search algorithm (SHAPER) described in Algorithm 1.

Following the strategies of PAS and PAM, the circuit is first divided into multiple k -qubit blocks and then resynthesis takes place at each block to get the best permutation with respect to all possible topologies as described in Section 2.3. Here, instead of considering different topologies for resynthesis, SHAPER only needs to care about all-to-all topology as the block can only be executed when all ions are in the same trap which yields an all-to-all connectivity. Consequently, different from SABRE, the front layer F of SHAPER contains k -qubit blocks. However, SHAPER still

Algorithm 1 SHAPER

```

1: INPUT Front layer  $F$ , Circuit  $C$ , ion assignment  $\Phi$ , distance
   matrix  $D$ , position graph  $G_p$ 
2: OUTPUT Instruction list  $\mathcal{I}$ , final ion assignment  $\Phi'$ 
3:  $\mathcal{I} \leftarrow []$ 
4: while  $F \neq \emptyset$  do
5:    $executable\_list \leftarrow \emptyset$ 
6:   Check through  $F$  to obtain all executable blocks
7:   if  $executable\_list \neq \emptyset$  then
8:     for circuit block  $B$  in  $executable\_list$  do
9:       Find the best permutation  $\pi$  of block  $B$ 
10:      Apply  $\pi$  to  $B$ 
11:      Update ion assignment  $\Phi$  with  $\pi$ 
12:      Update  $F$  with successors of executed blocks
13:     end for
14:   else
15:      $move\_scores \leftarrow []$ 
16:     Compute extended set  $E \leftarrow extended\_set(F, C)$ 
17:      $possible\_moves \leftarrow obtain\_moves(\Phi, G_p)$ 
18:     for  $move$  in  $possible\_moves$  do
19:       Update ion assignment  $\Phi$  with  $move$  as  $\Phi_{move}$ 
20:        $move\_scores[move] \leftarrow H(F, E, \Phi_{move}, D, G_p)$ 
21:     end for
22:     Select  $best\_move \leftarrow \arg \min (move\_scores)$ 
23:     if No  $best\_move$  or detected repeated path then
24:       Escape local minima with Algorithm 2
25:     else
26:       Update  $\Phi$  with  $best\_move$ 
27:       Append  $move$  to  $\mathcal{I}$ 
28:     end if
29:   end if
30: end while

```

maintains the same sliding framework where we scan the entire circuit from the front layer until the end and try to find the best move that enables all blocks to be executable.

Instead of using the mapping as in the superconducting system, we make use of ion assignment Φ which reflects the mapping of logical qubits to positions from the position graph as details in 4.2. This assignment reflects the current state of all ions within the system and demonstrates the hard constraints of the system while combining them with the position graph. Here the distance matrix D contains all costs to shuttle between pairs of positions in the position graph. This is calculated using Floyd-Warshall's algorithm [11].

The SHAPER algorithm constantly checks if F is empty (termination condition). The internal loops first check if any block in F is executable with respect to the current ion assignment Φ and the QCCD system. If there are executable gates, F finds the best permutation π for the block from the resynthesis, removes it from F , and adds the successor gate if all the dependencies are resolved (executed). Otherwise, if there is no executable block in F , we try to find the best transition (shuttling operation) for all the blocks in the front and extended layers. Here, the extended set includes successor gates from the front layer and the best permutation is calculated by the number of two-qubit gates as in [38] for simplicity.

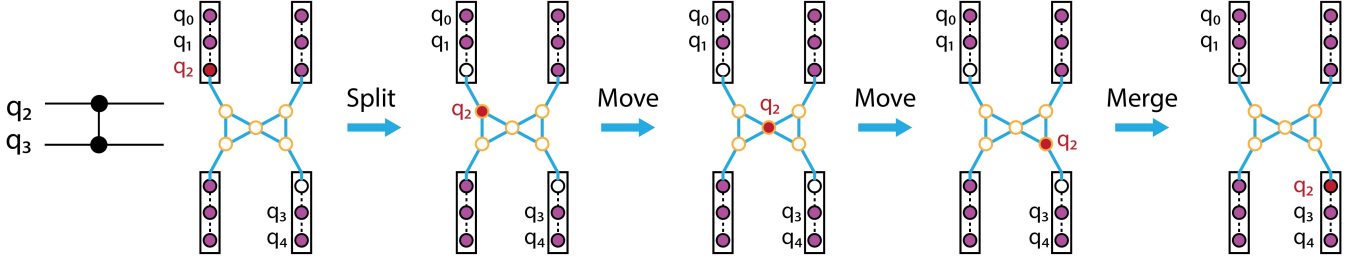


Figure 6: State of position graph after shuttling operations. As the two-qubit gate acted on q_2 and q_3 , the transition is reflected by the change of state of the position graph. Whenever q_2 is moved through a shuttling operation, the position graph fully captures the effect (occupied the space).

The scoring of the shuttling operation or move is different and more complex than that of the SWAP-based one, as the qubits must be near each other and in the same trap. Therefore, we propose the cost of shuttling in equation 7 which contains two parts, namely, \mathcal{F} for the blocks in the front layer and \mathcal{E} for the blocks in the extending set. This gives us a better look-ahead ability (can be adjusted with weight W_E). In both formulations of \mathcal{F} and \mathcal{E} , the first term indicates the maximum distance w.r.t to position graph between all pairs of qubits from the block B . Here we decide to use the maximum pairwise distance to not make the optimization landscape rougher. As an example, if considering the sum of all pairwise distances, if most qubits are near each other and there exists a faraway qubit, the optimization landscape becomes plateaus in most of the directions. For the second term in the formulation, we take the sum of all qubit positions to its nearest executable trap to ensure there exists a penalty term to force the qubits to move to the executable traps.

We use $d(p) = \min_{T_i \in \mathcal{T}} d_{T_i}(p)$ to denote the distance from position p to the nearest trap. The distance from position p to trap T_i , $d_{T_i}(p)$, is defined as follows: if trap T_i has free space then $d_{T_i}(p) = \min_{space \in T_i} (D[p][space])$; otherwise, $d_{T_i}(p) = \infty$. This formulation does not just inform how the next move contributes to gate execution but also implies the state of the system. For example, when all traps are crowded and some ions need to move to another trap, the split operation to move an ion from the trap gives the best cost.

$$\begin{aligned}
 \mathcal{F} &= \frac{1}{|F|} \sum_{B \in F} \left[\max_{q_i, q_j \in B} D[\Phi(q_i)][\Phi(q_j)] + \sum_{q_i \in B} d(\Phi(q_i)) \right] \\
 \mathcal{E} &= \frac{W_E}{|E|} \sum_{B \in E} \left[\max_{q_i, q_j \in B} D[\Phi(q_i)][\Phi(q_j)] + \sum_{q_i \in B} d(\Phi(q_i)) \right] \quad (7) \\
 \mathbf{H} &= \mathcal{F} + \mathcal{E},
 \end{aligned}$$

where W_E is the adjustable weight for the extended set and $\Phi(q_i)$ denotes position of qubit q_i in block B on G_p .

The scoring formulation from Equation 7 contains many local minima that can easily lead to a hold in our algorithm. Moreover, the SABRE algorithm is known to produce local minima and ways to escape from them. Therefore, we introduce a local-min resolution in

5.2 to help us escape from those local minima and avoid unnecessary moves.

After performing shuttling operations to enable gate execution, we continue the loop until the front layer is empty. This indicates we have already traveled one pass through the circuit. By doing this pass again but in a reverse manner (perform SHAPER but with the circuit flipped), we end an initial mapping of ion assignment for the original circuit. This is usually called the layout process [45].

5.2 Escaping local minimum

As the SHAPER optimization landscape is rugged, we need to help SHAPER escape the local minima while orchestrating the ions around, which is described in Algorithm 2. Here the block B is given as input and the physical positions of each logical qubit from block B are retrieved through ion assignment Φ .

After this, the trap T is selected with respect to the distance (shortest path) and path congestion (demonstrating how hard it is to move the ion to the trap space) when orchestrating the ions to the trap space. Then, the order of ions χ is also decided based on the same criteria for selecting trap T , where the first ion to be moved to trap T is the one with the minimum cost (shuttling time).

After selecting the trap and ion order, the algorithm starts with finding the shortest path from $\Phi(q_i)$ to the allocated trap space T called $P_{\Phi(q_i) \rightarrow T}$ (this can be done through Dijkstra's algorithm [16]). If the selected trap T is filled with ions, we try to release some space with *resolve_congestion* by moving the ions at the endpoint of trap T , denoted as $EP(T)$, out of the trap. When moving along the path, the ion can be stuck in a congestion (repeated moves or move in a circle) or deadlock (there is no possible move), the function *resolve_congestion* is called.

As shown in Algorithm 3, the recursive congestion resolution algorithm tries to resolve any conflict when trying to move p_1 to p_2 . Because p_1 can not move to p_2 ; p_2 must be occupied by an ion and both p_1 and p_2 must not be inside the trap zone (or else they can perform inner-swap). In the algorithm, p_2 's neighbors are considered to see if they are unoccupied and not lying on the main path $P_{\Phi(q_i) \rightarrow T}$. If any neighbor of p_2 satisfies the condition, ion at p_2 is moved to that space, and ion at p_1 is moved to p_2 which resolved the congestion. Otherwise, we perform a recursive call with p_2 and its neighbor $N(p_2)$ beside p_1 , by doing this, we try to

Algorithm 2 Escape Local Minimum

```
1: INPUT Block  $B$ , ion assignment  $\Phi$ , position graph  $G_p$ 
2: OUTPUT Instruction list  $\mathcal{I}$ , ion assignment  $\Phi'$ 
3:  $\mathcal{I} \leftarrow []$ 
4:  $physical\_position \leftarrow \Phi(q_i)$  for  $q_i \in B$ 
5: Find best trap  $T \in \mathbf{T}$  to move ions from  $physical\_position$  into.
6: Find the qubit order  $\chi$  to move
7: for qubit  $q_i$  in  $\chi$  do
8:   Find the shortest path  $P_{\Phi(q_i) \rightarrow T}$ 
9:   if there exist no space in  $T$  then
10:      $resolve\_congestion(EP(T), N(EP(T)), P_{\Phi(q_i) \rightarrow T}, \Phi)$ 
11:   end if
12:   for move  $P_{i \rightarrow i'}$  in  $P_{\Phi(q_i) \rightarrow T}$  do
13:     if there exists congestion in  $P_{i \rightarrow i'}$  then
14:        $resolve\_congestion(i, i', P_{\Phi(q_i) \rightarrow T}, \Phi)$  with Alg. 3
15:     else
16:       Perform move ( $i \rightarrow i'$ )
17:       Append move ( $i \rightarrow i'$ ) to  $\mathcal{I}$ 
18:     end if
19:   end for
20: end for
```

move the far-distance neighbor of p_2 away to create space for lower-distance neighbor and finally create space for p_2 to move out of the path. Note that this strategy can lead to a deadlock situation due to the presence of multiple ions outside of the trap zone. Therefore, we also enforce a mechanism to push every ion back to the nearest traps when the congestion rate on the shuttling path is too high.

Algorithm 3 Resolve congestion

```
INPUT Positions  $p_1$  and  $p_2$ , path  $P_{\Phi(I) \rightarrow T}$ , ion assignment  $\Phi$ 
OUTPUT Instruction List  $\mathcal{I}$ , Ion Assignment  $\Phi'$ 
 $\mathcal{I} \leftarrow []$ 
Obtain neighbors of  $p_2 \leftarrow N(p_2)$ . Remove  $p_1$  out of the list.
 $moved\_flag \leftarrow \text{FALSE}$ 
for  $p$  in  $N(p_2)$  do
  if  $\Phi(p) == \emptyset$  and  $p \notin P_{\Phi(I) \rightarrow T}$  then
    Perform move ( $p_2 \rightarrow p$ )
    Append move ( $p_2 \rightarrow p$ ) to  $\mathcal{I}$ .
     $moved\_flag \leftarrow \text{TRUE}$ 
    BREAK
  end if
end for
if  $moved\_flag$  then
  Perform move ( $p_1 \rightarrow p_2$ )
  Append move ( $p_1 \rightarrow p_2$ ) to  $\mathcal{I}$ .
else
   $resolve\_congestion(p_2, N(p_2), P_{\Phi(I) \rightarrow T})$ 
end if
```

For better illustration, we show an example in Figure 7 of how our algorithm to resolve the congestions works. In this case, we want to move q_2 to the same trap zone of q_3 , however, the trap containing q_3 is already full. Therefore, the first step is to move the ion at the trap's endpoint q_5 out of the trap, then we start moving q_2

Algorithm/Applications	# qubits	# 2-qubit gates
QAOA	16	168
QAOA	20	246
QFT	16	252
QFT	20	353
Quantum Volume	16	72
Quantum Volume	20	90
TFIM	16	199
TFXY	16	236

Table 1: Details about benchmark circuit for the experiments between SHAPER and QCCDSim.

toward the designated trap. When going to reach the trap, we can see that there is congestion caused by q_5 , this can be easily solved by moving q_5 out of the path and toward another trap. Finally q_2 successfully merges into the same trap with q_3 and gate acting on (q_2, q_3) is executed.

6 EVALUATION

6.1 Experimental setup

The experiments are performed on well-known quantum algorithms and applications ranging from 16 to 20 qubits. Table 1 details all the benchmark circuits. The Quantum Approximate Optimization Algorithm (QAOA) [19] is a variational algorithm broadly applicable on NISQ devices for combinatorial optimization problems. The Quantum Fourier Transform (QFT) [47] is a common quantum circuit for designing larger algorithms such as the Quantum Phase Estimation [1]. The Quantum Volume (QV) circuits are commonly used as a benchmark for evaluating quantum hardware performance [12]. The Transverse Field Ising Model (TFIM) and Transverse Field XY (TFXY) circuits are quantum circuits for Hamiltonian simulation [61]. These are crucial simulation models for many near-term applications using quantum computing. Here the QFT, QV, and QAOA are generated using the Qiskit framework [27]. In particular, QAOA is generated based on Erdős-Rényi graph with edge probability equal to 0.3. The TFIM and TFXY circuits were generated by the F3C++ compiler [32].

We developed SHAPER in Python 3.11 as a BQSKit [69] extension. We evaluated the SHAPER algorithm against the state-of-the-art shuttling algorithm, QCCDSim [45]. The evaluation was performed on an AMD EPYC 7702 processor with 1TB of main memory. QCCDSim only supports circuits already transpiled to a gateset containing CNOTs. As a result, we transpiled all input circuits with BQSKit to this gateset to enable a comparison. Our source code and results are available at [link will be added here upon acceptance].

6.2 Experimental results

We compare our method with the QCCDSim compiler [45]. We record two metrics: the final compiled circuit execution time as well as the time needed for compilation. We chose QCCDSim due to its capability to derive a near-optimal shuttling schedule for 2D QCCD architecture. Moreover, it is the only available framework that works with variable architectures.

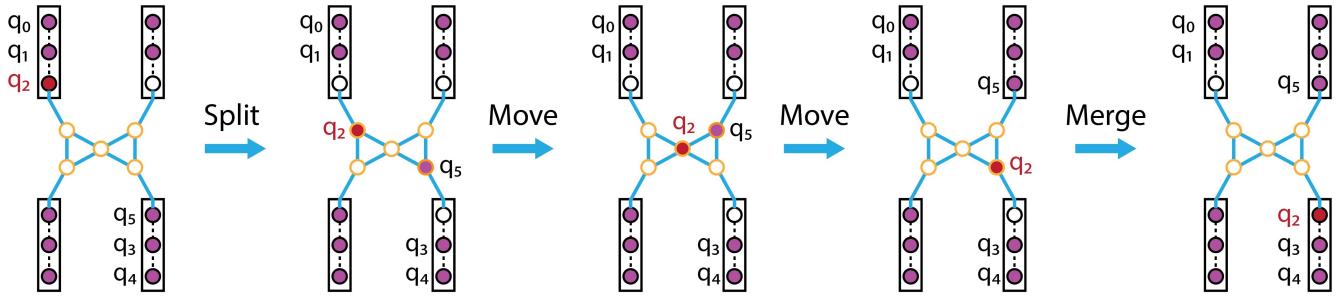


Figure 7: When moving q_2 toward the same trap zone with q_3 , there is congestion caused by q_5 . Here we show how our algorithm resolves this congestion by moving q_5 out of the trap. As different shuttling operations can be performed at the same time, the figure shows the shuttling operations of q_2 and q_5 parallelly.

The results of SHAPER and QCCDSim are presented in Table 2. We evaluated two different QCCD architectures, H and $G2x3$. The H architecture has been pictured previously in Figure 1. The $G2x3$ architecture is created from the H by adding another column of traps and changing the now-middle Y-junction to an X-junction. We vary the maximum ions per trap and report the shuttling time in microseconds. QCCDSim is deterministic and only runs once. However, there is randomness in our initial layout process, and as a result, we run SHAPER five times and present the best result. *QCCDSim fails to complete in situations with high congestion; these cases are marked with an X in the table.* In particular, QCCDSim fails when the circuit width matches the total trap capacity. These scenarios provide no extra positions in the trap, creating large congestion in the junctions. In all of these cases, SHAPER successfully returned a valid shuttling sequence which is critical for quantum compilation, not to mention its scalability.

SHAPER finds compiled sequences on average 1.15 times shorter when only considering the benchmarks with results for both algorithms. In the best-case trial, we produced a sequence that was 1.69 times shorter. The standard deviation of the results from SHAPER is around 4.1%. Out of the 32 trials, we produced a sequence that was shorter in 29 cases. The 3 cases where SHAPER was worse than QCCDSim are because of a poor initial layout which is a great direction for future work. SHAPER takes an average of 270.25 seconds to run across all the benchmarks, while QCCDSim takes 1.3 seconds on average over those benchmarks that were completed. This discrepancy is mainly due to the resynthesis step from PAM. Other mapping algorithms that may use the position graph will not experience these compile times. However, we stress that QCCDSim was not able to complete many of the available benchmarks, especially when the benchmark size matched the amount of available space from traps.

7 RELATED WORK

There has been significant research in the compilation of superconducting qubit systems. In [34, 38, 62, 72], the authors were concerned with finding the best mapping based on the original circuit. In [13, 35, 70], the goal was to find the best-synthesized circuit concerning the hardware connectivity graph by performing

synthesis. Different techniques (e.g., machine learning) for finding the best-synthesized circuit for the connectivity graph are also well-studied [17, 43, 71]. A more detailed review of quantum compilation and synthesis of superconducting-based systems can be found in [23]. Apart from the academic researchers, open-source compilation tools for superconducting devices from companies such as IBM’s Qiskit [27], Google’s Cirq [15] and Rigetti’s Quilc [63] are also well-known in the community.

In the opposite situation, the QCCD-based TI system, known for its robustness and is the candidate for fault-tolerant quantum computation [21, 28, 46], does not have much to offer. Prior work on shuttling-trapped ion prefers to evaluate the hardware architectures while using some compilation schemes [6, 45, 59]. There are also prior works that try to solve the circuit mapping problem for shuttling-based TI systems such as [18, 50, 57, 58, 66]. However, each has its downside, [18, 66] only considers minimizing shuttling operations in one dimension system (linear segment). The works [57, 58] attempt to perform the circuit optimization for the operations but the approach is hardware-agnostic. They simplify the hardware architecture into a memory zone and a processing zone. Their memory zone is a geometric grid, composed of uniform blocks and the main target is to move the ions from the memory zone to the processing zone while resolving congestion by cycle-based shuttling. This simplification can not capture the big picture yielded by 2D QCCD architecture. For example, given many executable traps that we can use, the shuttling problem is not simply to move the ions to a specific processing zone but also to find the optimal trap zone for each ion. Moreover, this simplification fails to catch the congestion caused by having multiple trap zones.

In [50], the authors attempt to find the best initial mapping from the device’s architecture but do not solve the orchestrating problem. Besides direct attempts to solve the circuit mapping problem as listed, there are efforts to solve the whole compilation framework. For example, [33] tries to find the best-compiled quantum circuit to run with TI hardware but does not touch the shuttling operations, while [56] gives an optimized version of compiled-circuit and shuttling sequences but only deals with one-dimensional architecture.

In conclusion, to bridge these gaps, our work (1) enriches the works of QCCD-based TI compilation by bridging the difference

Benchmark Circuit	Arch.	# trap	Ions/trap	SHAPER (μ s)	Runtime (s)	QCCDSim (μ s)	Runtime (s)
QAOA16	H	4	4	28352	112.8	X	X
			5	31396	146.76	34790	0.93
	G2x3	6	3	33026	125.06	X	X
			4	33246	182.77	39063	0.93
QuantumVolume_16	H	4	4	9245	233.37	X	X
			5	8733	266.41	11162	0.3
	G2x3	6	3	9457	243.31	X	X
			4	10001	317.81	13535	0.31
QFT_16	H	4	4	43610	145.8	X	X
			5	42063	162.89	45488	1.57
	G2x3	6	3	42744	155.60	X	X
			4	41684	208.65	36329	1.55
TFIM_n16_s100	H	4	4	35509	133.89	X	X
			5	33126	145.65	36707	0.69
	G2x3	6	3	34178	139.69	X	X
			4	34956	259.2	42251	0.73
TFXY_n16_s100	H	4	4	39918	298.97	X	X
			5	39401	364.14	27135	1.21
	G2x3	6	3	45999	309.54	X	X
			4	38299	439.36	45998	1.11
QAOA_20	H	4	5	45981	184.89	X	X
			6	50113	260.8	55940	2.31
	G2x3	6	4	44829	220.31	X	X
			5	50010	740.42	51266	2.37
QuantumVolume_20	H	4	5	13657	259.05	X	X
			6	13307	308.87	17674	0.39
	G2x3	6	4	13704	318.97	X	X
			5	12971	574.15	15612	0.38
QFT_20	H	4	5	56705	229.44	X	X
			6	65029	278.48	56281	2.96
	G2x3	6	4	61582	269.34	X	X
			5	68521	611.66	70134	3

Table 2: Direct comparison between SHAPER and QCCDSim for different circuits and hardware architectures. Here the shuttling time is in micro-seconds (μ s) while the compile time is in seconds (s). An X indicates a failure in resolving the shuttling problem for a specific configuration.

between TI and superconducting-based literature with the *position graph* abstraction, (2) finds the best-compiled circuit on the given two-dimension architecture with executable traps, loading zones, shuttling paths and junctions, (3) proves that the *position graph* abstraction works well by coming up with SHAPER to orchestrate the ions with shuttling operations, and finds the best-permuted circuit while resolving the congestion and deadlock problems.

8 DISCUSSION AND CONCLUSION

Better mapping algorithm based on the position graph abstraction. In this work, we aimed to bridge the gap between the well-studied qubit allocation [62] and the routing problem of the superconducting system with the shuttling-based compilation through the position graph abstraction. To prove this point, we introduced the SHuttling-Aware PERmutative search algorithm (SHAPER) which

is inspired by the state-of-the-art SABRE [34] and the permutation-aware mapping (PAM) [38]. Moreover, as many routing and mapping algorithms share a similar approach with SABRE [37, 48, 49, 51, 73], we believe that despite having more constraints and the existence of congestion, those methods can be applied to the TI system through our novel position graph. We believe that, while demonstrating high quality, our heuristic mapping and scheduling algorithms are still not optimal and there should be better innovative approaches using the position graph abstraction.

Scalability potential of the position graph for QCCD-based TI system. We argue that the abstraction of the position graph is very scalable and is not only designed for the current state of QCCD-based TI systems. First, the trap zone representation is linear to fit the current state-of-the-art system [14, 44, 64], however, this can be easily adapted to other types of 2D trap ion arrays in different lattice configurations such as hexagonal [65], triangular [40] and square

[8]. Moreover, the current state of QCCD systems usually considers Y-junction (T-junction) and X-junction [5, 7, 25] (corresponding to 3-degree and 4-degree junctions respectively), while the position graph abstraction can express even higher d -degree junction through the construction of the complete graph. Finally, we also argue that the position graph will also be expressible even if the QCCD-based TI system is not planar and becomes 3D architecture such as flip-chip from superconducting qubits [10]. This is because we can derive a position graph for each chip layer and put them on top of each other.

ACKNOWLEDGMENTS

B.B and I.S are supported with funding from the Defense Advanced Research Projects Agency (DARPA) under the ONISQ program. E.Y. is supported by the U.S. Department of Energy, Office of Science, Office of Advanced Scientific Computing Research under Contract No. DE-AC05-00OR22725 through the Accelerated Research in Quantum Computing Program MACH-Q project.

REFERENCES

- [1] Daniel S Abrams and Seth Lloyd. 1999. Quantum algorithm providing exponential speed increase for finding eigenvalues and eigenvectors. *Physical Review Letters* 83, 24 (1999), 5162.
- [2] Christopher J Ballance, Thomas P Harty, Nibert M Linke, Martin A Sepiol, and David M Lucas. 2016. High-fidelity quantum logic gates using trapped-ion hyperfine qubits. *Physical review letters* 117, 6 (2016), 060504.
- [3] Debjyoti Bhattacharjee, Abdullah Ash Saki, Mahabubul Alam, Anupam Chattopadhyay, and Swaroop Ghosh. 2019. MUQUT: Multi-constraint quantum circuit mapping on NISQ computers. In *2019 IEEE/ACM international conference on computer-aided design (ICCAD)*. IEEE, 1–7.
- [4] Jacob Biamonte, Peter Wittek, Nicola Pancotti, Patrick Rebentrost, Nathan Wiebe, and Seth Lloyd. 2017. Quantum machine learning. *Nature* 549, 7671 (2017), 195–202.
- [5] RB Blakestad, C Ospelkaus, AP VanDevender, JM Amini, Joseph Britton, Dietrich Leibfried, and David J Wineland. 2009. High-fidelity transport of trapped-ion qubits through an X-junction trap array. *Physical review letters* 102, 15 (2009), 153002.
- [6] Kenneth R Brown, Jungsang Kim, and Christopher Monroe. 2016. Co-designing a scalable quantum computer with trapped atomic ions. *npj Quantum Information* 2, 1 (2016), 1–10.
- [7] Colin D Bruzewicz, John Chiaverini, Robert McConnell, and Jeremy M Sage. 2019. Trapped-ion quantum computing: Progress and challenges. *Applied Physics Reviews* 6, 2 (2019).
- [8] Colin D Bruzewicz, Robert McConnell, John Chiaverini, and Jeremy M Sage. 2016. Scalable loading of a two-dimensional trapped-ion array. *Nature communications* 7, 1 (2016), 13005.
- [9] Yudong Cao, Jonathan Romero, Jonathan P Olson, Matthias Degroote, Peter D Johnson, Mária Kieferová, Ian D Kivlichan, Tim Menke, Borja Peropadre, Nicolas PD Sawaya, Sukin Sim, Libor Veis, and Alan Aspuru-Guzik. 2019. Quantum chemistry in the age of quantum computing. *Chemical reviews* 119, 19 (2019), 10856–10915.
- [10] CR Conner, A Bienfait, H-S Chang, M-H Chou, É Dumur, J Grebel, GA Peairs, RG Povey, H Yan, YP Zhong, et al. 2021. Superconducting qubits in a flip-chip architecture. *Applied Physics Letters* 118, 23 (2021).
- [11] Thomas H. Cormen, Charles E. Leiserson, Ronald L. Rivest, and Clifford Stein. 2009. *Introduction to Algorithms* (3rd ed.). MIT Press. 693–700 pages. Section on the Floyd-Warshall algorithm.
- [12] Andrew W Cross, Lev S Bishop, Sarah Sheldon, Paul D Nation, and Jay M Gambetta. 2019. Validating quantum computers using randomized model circuits. *Physical Review A* 100, 3 (2019), 032328.
- [13] Marc G Davis, Ethan Smith, Ana Tudor, Koushik Sen, Irfan Siddiqi, and Costin Iancu. 2020. Towards optimal topology aware quantum circuit synthesis. In *2020 IEEE International Conference on Quantum Computing and Engineering (QCE)*. IEEE, 223–234.
- [14] Robert D Delaney, Lucas R Sletten, Matthew J Cich, Brian Estey, Maya I Fabrikant, David Hayes, Ian M Hoffman, James Hostetter, Christopher Langer, Steven A Moses, et al. 2024. Scalable Multispecies Ion Transport in a Grid-Based Surface-Electrode Trap. *Physical Review X* 14, 4 (2024), 041028.
- [15] Cirq Developers. 2024. *Cirq*. <https://doi.org/10.5281/zenodo.11398048>
- [16] Edsger W Dijkstra. 2022. A note on two problems in connexion with graphs. In *Edsger Wybe Dijkstra: his life, work, and legacy*. 287–290.
- [17] Trong Duong, Sang T Truong, Minh Tam, Bao Bach, Ju-Young Ryu, and June-Koo Kevin Rhee. 2022. Quantum neural architecture search with quantum circuits metric and bayesian optimization. *arXiv preprint arXiv:2206.14115* (2022).
- [18] Jonathan Durandau, Janis Wagner, Frédéric Mailhot, Charles-Antoine Brunet, Ferdinand Schmidt-Kaler, Ulrich Poschinger, and Yves Bérubé-Lauzière. 2023. Automated generation of shuttling sequences for a linear segmented ion trap quantum computer. *Quantum* 7 (2023), 1175.
- [19] Edward Farhi, Jeffrey Goldstone, and Sam Gutmann. 2014. A quantum approximate optimization algorithm. *arXiv preprint arXiv:1411.4028* (2014).
- [20] Caroline Figgatt. 2023. Dancing with Ions: Inside the Quantum Quantum Computer. In *APS March Meeting Abstracts (APS Meeting Abstracts, Vol. 2023)*. Article W50.005, W50.005 pages.
- [21] Michael Foss-Feig, Guido Pagano, Andrew C Potter, and Norman Y Yao. 2024. Progress in trapped-ion quantum simulation. *Annual Review of Condensed Matter Physics* 16 (2024).
- [22] John P Gaebler, Ting Rei Tan, Yiheng Lin, Y Wan, Ryan Bowler, Adam C Keith, Scott Glancy, Kevin Coakley, Emanuel Knill, Dietrich Leibfried, et al. 2016. High-fidelity universal gate set for be 9+ ion qubits. *Physical review letters* 117, 6 (2016), 060505.
- [23] Yan Ge, Wu Wenjie, Chen Yuheng, Pan Kaisen, Lu Xudong, Zhou Zixiang, Wang Yuhuan, Wang Ruocheng, and Yan Junchi. 2024. Quantum circuit synthesis and compilation optimization: Overview and prospects. *arXiv preprint arXiv:2407.00736* (2024).
- [24] M Gutiérrez, M Müller, and Alejandro Bermúdez. 2019. Transversality and lattice surgery: Exploring realistic routes toward coupled logical qubits with trapped-ion quantum processors. *Physical Review A* 99, 2 (2019), 022330.
- [25] WK Hensinger, S Olmschenk, D Stick, D Hucul, M Yeo, Mark Acton, L Deslauriers, C Monroe, and J Rabchuk. 2006. T-junction ion trap array for two-dimensional ion shuttling, storage, and manipulation. *Applied Physics Letters* 88, 3 (2006).
- [26] Dylan Herman, Cody Googin, Xiaoyuan Liu, Yue Sun, Alexey Galda, Ilya Saffro, Marco Pistoia, and Yuri Alexeev. 2023. Quantum computing for finance. *Nature Reviews Physics* 5, 8 (2023), 450–465.
- [27] Ali Javadi-Abhari, Matthew Treinish, Kevin Krsulich, Christopher J. Wood, Jake Lishman, Julien Gacon, Simon Martiel, Paul D. Nation, Lev S. Bishop, Andrew W. Cross, Blake R. Johnson, and Jay M. Gambetta. 2024. Quantum computing with Qiskit. <https://doi.org/10.48550/arXiv.2405.08810> arXiv:2405.08810 [quant-ph]
- [28] Mingyu Kang, Hanggai Nuomin, Sutirtha N Chowdhury, Jonathon L Yuly, Ke Sun, Jacob Whitlow, Jesús Valdiviezo, Zhendian Zhang, Peng Zhang, David N Beratan, et al. 2024. Seeking a quantum advantage with trapped-ion quantum simulations of condensed-phase chemical dynamics. *Nature Reviews Chemistry* (2024), 1–19.
- [29] David Kielpinski, Chris Monroe, and David J Wineland. 2002. Architecture for a large-scale ion-trap quantum computer. *Nature* 417, 6890 (2002), 709–711.
- [30] Morten Kjaergaard, Mollie E Schwartz, Jochen Braumüller, Philip Krantz, Joel I-J Wang, Simon Gustavsson, and William D Oliver. 2020. Superconducting qubits: Current state of play. *Annual Review of Condensed Matter Physics* 11, 1 (2020), 369–395.
- [31] Jens Koch, Terri M Yu, Jay Gambetta, Andrew A Houck, David I Schuster, Johannes Majer, Alexandre Blais, Michel H Devoret, Steven M Girvin, and Robert J Schoelkopf. 2007. Charge-insensitive qubit design derived from the Cooper pair box. *Physical Review A—Atomic, Molecular, and Optical Physics* 76, 4 (2007), 042319.
- [32] Efehan Kökcü, Daan Camps, Lindsay Bassman Oftelie, James K Freericks, Wibe A de Jong, Roel Van Beeumen, and Alexander F Kemper. 2022. Algebraic compression of quantum circuits for Hamiltonian evolution. *Physical Review A* 105, 3 (2022), 032420.
- [33] Fabian Kreppel, Christian Melzer, Diego Olvera Millán, Janis Wagner, Janine Hilder, Ulrich Poschinger, Ferdinand Schmidt-Kaler, and André Brinkmann. 2023. Quantum circuit compiler for a shuttling-based trapped-ion quantum computer. *Quantum* 7 (2023), 1176.
- [34] Gushu Li, Yufei Ding, and Yuan Xie. 2019. Tackling the qubit mapping problem for NISQ-era quantum devices. In *Proceedings of the twenty-fourth international conference on architectural support for programming languages and operating systems*. 1001–1014.
- [35] Chia-Chun Lin, Amlan Chakrabarti, and Niraj K Jha. 2013. FTQLS: Fault-tolerant quantum logic synthesis. *IEEE Transactions on very large scale integration (VLSI) systems* 22, 6 (2013), 1350–1363.
- [36] Norbert M Linke, Dmitri Maslov, Martin Roetteler, Shantanu Debnath, Caroline Figgatt, Kevin A Landsman, Kenneth Wright, and Christopher Monroe. 2017. Experimental comparison of two quantum computing architectures. *Proceedings of the National Academy of Sciences* 114, 13 (2017), 3305–3310.
- [37] Ji Liu, Peiyi Li, and Huiyang Zhou. 2022. Not all swaps have the same cost: A case for optimization-aware qubit routing. In *2022 IEEE International Symposium on High-Performance Computer Architecture (HPCA)*. IEEE, 709–725.

- [38] Ji Liu, Ed Younis, Mathias Weiden, Paul Hovland, John Kubiatowicz, and Costin Iancu. 2023. Tackling the qubit mapping problem with permutation-aware synthesis. In *2023 IEEE International Conference on Quantum Computing and Engineering (QCE)*, Vol. 1. IEEE, 745–756.
- [39] M Malinowski, DTC Alcock, and CJ Ballance. 2023. How to wire a 1000-qubit trapped-ion quantum computer. *PRX Quantum* 4, 4 (2023), 040313.
- [40] Manuel Mielenz, Henning Kalis, Matthias Wittermer, Frederick Hakeberg, Ulrich Warring, Roman Schmied, Matthew Blain, Peter Maunz, David L Moehring, Dietrich Leibfried, et al. 2016. Arrays of individually controlled ions suitable for two-dimensional quantum simulations. *Nature communications* 7, 1 (2016), ncomms11839.
- [41] Abtin Molavi, Amanda Xu, Martin Diges, Lauren Pick, Swamit Tannu, and Aws Albarghouthi. 2022. Qubit mapping and routing via MaxSAT. In *2022 55th IEEE/ACM international symposium on Microarchitecture (MICRO)*. IEEE, 1078–1091.
- [42] Carmelo Mordini, Alfredo Ricci Vasquez, Yuto Motohashi, Mose Müller, Maciej Malinowski, Chi Zhang, Karan K Mehta, Daniel Kienzler, and Jonathan P Home. 2024. Multi-zone trapped-ion qubit control in an integrated photonics QCCD device. *arXiv preprint arXiv:2401.18056* (2024).
- [43] Lorenzo Moro, Matteo GA Paris, Marcello Restelli, and Enrico Prati. 2021. Quantum compiling by deep reinforcement learning. *Communications Physics* 4, 1 (2021), 178.
- [44] Steven A Moses, Charles H Baldwin, Michael S Allman, R Ancona, L Ascarrunz, C Barnes, J Bartolotta, B Bjork, P Blanchard, M Bohn, et al. 2023. A race-track trapped-ion quantum processor. *Physical Review X* 13, 4 (2023), 041052.
- [45] Prakash Murali, Dripto M Debroy, Kenneth R Brown, and Margaret Martonosi. 2020. Architecting noisy intermediate-scale trapped ion quantum computers. In *2020 ACM/IEEE 47th Annual International Symposium on Computer Architecture (ISCA)*. IEEE, 529–542.
- [46] Prakash Murali, Norbert Matthias Linke, Margaret Martonosi, Ali Javadi Abhari, Nhung Hong Nguyen, and Cynthia Huerta Alderete. 2019. Full-stack, real-system quantum computer studies: Architectural comparisons and design insights. In *Proceedings of the 46th International Symposium on Computer Architecture*. 527–540.
- [47] Michael A Nielsen and Isaac L Chuang. 2001. *Quantum computation and quantum information*. Vol. 2. Cambridge university press Cambridge.
- [48] Siyuan Niu, Adrien Suau, Gabriel Staffelbach, and Aida Todri-Sanial. 2020. A hardware-aware heuristic for the qubit mapping problem in the nisq era. *IEEE Transactions on Quantum Engineering* 1 (2020), 1–14.
- [49] Siyuan Niu and Aida Todri-Sanial. 2023. Enabling multi-programming mechanism for quantum computing in the NISQ era. *Quantum* 7 (2023), 925.
- [50] Anabel Ovide, Daniele Cuomo, and Carmen G Almudever. 2024. Scaling and assigning resources on ion trap QCCD architectures. *arXiv preprint arXiv:2408.00225* (2024).
- [51] Sunghye Park, Daeyeon Kim, Minhyuk Kweon, Jae-Yoon Sim, and Seokhyeong Kang. 2022. A fast and scalable qubit-mapping method for noisy intermediate-scale quantum computers. In *Proceedings of the 59th ACM/IEEE Design Automation Conference*. 13–18.
- [52] Juan M Pino, Jennifer M Dreiling, Caroline Figgatt, John P Gaebler, Steven A Moses, MS Allman, CH Baldwin, Michael Foss-Feig, David Hayes, Karl Mayer, et al. 2021. Demonstration of the trapped-ion quantum CCD computer architecture. *Nature* 592, 7853 (2021), 209–213.
- [53] Quantinuum. 2023. Quantinuum Unveils Accelerated Roadmap to Achieve Universal Fault-Tolerant Quantum Computing by 2030. <https://www.quantinuum.com/press-releases/quantinuum-unveils-accelerated-roadmap-to-achieve-universal-fault-tolerant-quantum-computing-by-2030> Accessed: 2024-11-12.
- [54] Quantinuum. 2024. Quantinuum Systems. <https://www.quantinuum.com/products-solutions/quantinuum-systems> Accessed: 2024-11-22.
- [55] Stig Elkjær Rasmussen, Kasper Sangild Christensen, Simon Panyella Pedersen, Lasse Bjørn Kristensen, Thomas Bækkegaard, Niels Jakob Søe Loft, and Nikolaj Thomas Zinner. 2021. Superconducting circuit companion—an introduction with worked examples. *PRX Quantum* 2, 4 (2021), 040204.
- [56] Abdullah Ash Saki, Rasit Onur Topaloglu, and Swaroop Ghosh. 2022. Muzzle the shuttle: efficient compilation for multi-trap trapped-ion quantum computers. In *2022 Design, Automation & Test in Europe Conference & Exhibition (DATE)*. IEEE, 322–327.
- [57] Daniel Schoenberger, Stefan Hillmich, Matthias Brandl, and Robert Wille. 2024. Shuttling for Scalable Trapped-Ion Quantum Computers. *arXiv preprint arXiv:2402.14065* (2024).
- [58] Daniel Schoenberger, Stefan Hillmich, Matthias Brandl, and Robert Wille. 2024. Using Boolean satisfiability for exact shuttling in trapped-ion quantum computers. In *2024 29th Asia and South Pacific Design Automation Conference (ASP-DAC)*. IEEE, 127–133.
- [59] Daniel Schoenberger, Stefan Hillmich, Matthias Brandl, and Robert Wille. 2024. Using Compiler Frameworks for the Evaluation of Hardware Design Choices in Trapped-Ion Quantum Computers. (2024).
- [60] Ruslan Shayduln, Hayato Ushijima-Mwesigwa, Christian FA Negre, Ilya Safro, Susan M Mniszewski, and Yuri Alexeev. 2019. A hybrid approach for solving optimization problems on small quantum computers. *Computer* 52, 6 (2019), 18–26.
- [61] Dongbin Shin, Hannes Hübener, Umberto De Giovannini, Hosub Jin, Angel Rubio, and Noejung Park. 2018. Phonon-driven spin-Floquet magneto-valleytronics in MoS₂. *Nature communications* 9, 1 (2018), 638.
- [62] Marcos Yukio Siraichi, Vinicius Fernandes dos Santos, Caroline Collange, and Fernando Magno Quintão Pereira. 2018. Qubit allocation. In *Proceedings of the 2018 international symposium on code generation and optimization*. 113–125.
- [63] Robert S Smith, Eric C Peterson, Mark G Skilbeck, and Erik J Davis. 2020. An open-source, industrial-strength optimizing compiler for quantum programs. *Quantum Science and Technology* 5, 4 (2020), 044001.
- [64] JD Sterk, MG Blain, M Delaney, R Haldli, E Heller, AL Holterhoff, T Jennings, N Jimenez, A Kozhanov, Z Meinelt, et al. 2024. Multi-junction surface ion trap for quantum computing. *arXiv preprint arXiv:2403.00208* (2024).
- [65] Robin C Sterling, Hwanjit Rattanasonti, Sebastian Weidt, Kim Lake, Prasanna Srinivasan, SC Webster, Michaël Kraft, and Winfried K Hensinger. 2014. Fabrication and operation of a two-dimensional ion-trap lattice on a high-voltage microchip. *Nature communications* 5, 1 (2014), 3637.
- [66] Wei-Hsiang Tseng, Yao-Wen Chang, and Jie-Hong Roland Jiang. 2024. Satisfiability Modulo Theories-Based Qubit Mapping for Trapped-Ion Quantum Computing Systems. In *Proceedings of the 2024 International Symposium on Physical Design*. 245–253.
- [67] Yukai Wu, Sheng-Tao Wang, and L-M Duan. 2018. Noise analysis for high-fidelity quantum entangling gates in an anharmonic linear paul trap. *Physical Review A* 97, 6 (2018), 062325.
- [68] Ed Younis and Costin Iancu. 2022. Quantum circuit optimization and transpilation via parameterized circuit instantiation. In *2022 IEEE International Conference on Quantum Computing and Engineering (QCE)*. IEEE, 465–475.
- [69] Ed Younis, Costin C Iancu, Wim Lavrijsen, Marc Davis, and Ethan Smith. 2021. *Berkeley quantum synthesis toolkit (bqskit) v1*. Technical Report. Lawrence Berkeley National Laboratory (LBNL), Berkeley, CA (United States).
- [70] Ed Younis, Koushik Sen, Katherine Yelick, and Costin Iancu. 2021. Qfast: Conflating search and numerical optimization for scalable quantum circuit synthesis. In *2021 IEEE International Conference on Quantum Computing and Engineering (QCE)*. IEEE, 232–243.
- [71] Yuan-Hang Zhang, Pei-Lin Zheng, Yi Zhang, and Dong-Ling Deng. 2020. Topological quantum compiling with reinforcement learning. *Physical Review Letters* 125, 17 (2020), 170501.
- [72] Pengcheng Zhu, Xueyun Cheng, and Zhijin Guan. 2020. An exact qubit allocation approach for NISQ architectures. *Quantum Information Processing* 19, 11 (2020), 391.
- [73] Pengcheng Zhu, Zhijin Guan, and Xueyun Cheng. 2020. A dynamic look-ahead heuristic for the qubit mapping problem of NISQ computers. *IEEE Transactions on Computer-Aided Design of Integrated Circuits and Systems* 39, 12 (2020), 4721–4735.